European Journal of Inorganic Chemistry

Supporting Information

# Ultrafast Near-Infrared Luminescence from Cyclometalated Iridium(III) Complexes with Indirubin as Ancillary Ligand

Kochan Sathyaseelan Bejoymohandas, Barbara Ventura, Andrea Baschieri, Andrea Mazzanti, Elisa Bandini, and Filippo Monti*

Supporting Information

# Ultrafast Near-Infrared Luminescence from Cyclometalated Iridium(III) Complexes with Indirubin as Ancillary Ligand

Kochan Sathyaseelan Bejoymohandas,[a] Barbara Ventura,[a] Andrea Baschieri,[a] Andrea Mazzanti,[b] Elisa Bandini,[a] and Filippo Monti*[a]

[a] Institute for Organic Synthesis and Photoreactivity (ISOF), National Research Council of Italy (CNR), Via P. Gobetti101, I-40129 Bologna (Italy). E-mail: filippo.monti@isof.cnr.it
[b] Department of Industrial Chemistry "Toso Montanari", University of Bologna, Via P. Gobetti 85, I-40129 Bologna (Italy).

***Contents*** ***Pages***

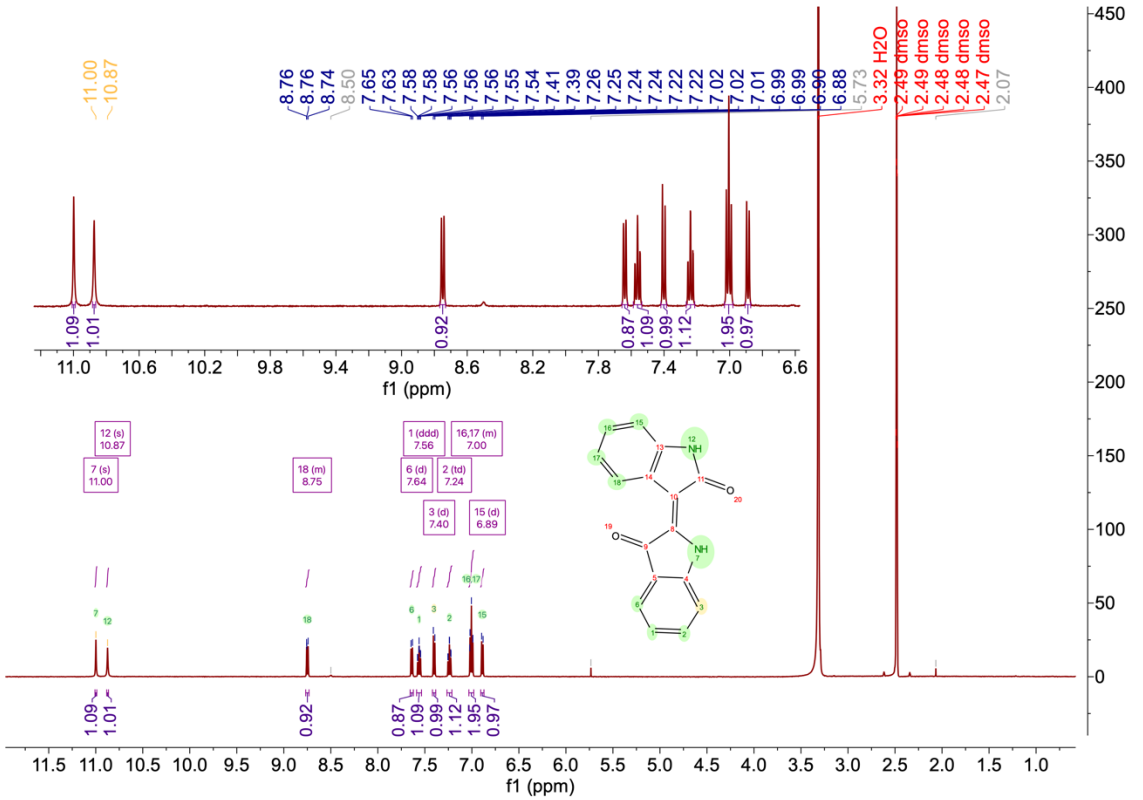


**Figure S1.** $^{1}$H-NMR spectrum of *(Z)-[2,3'-biindolinylidene]-2',3-dione* (indirubin).

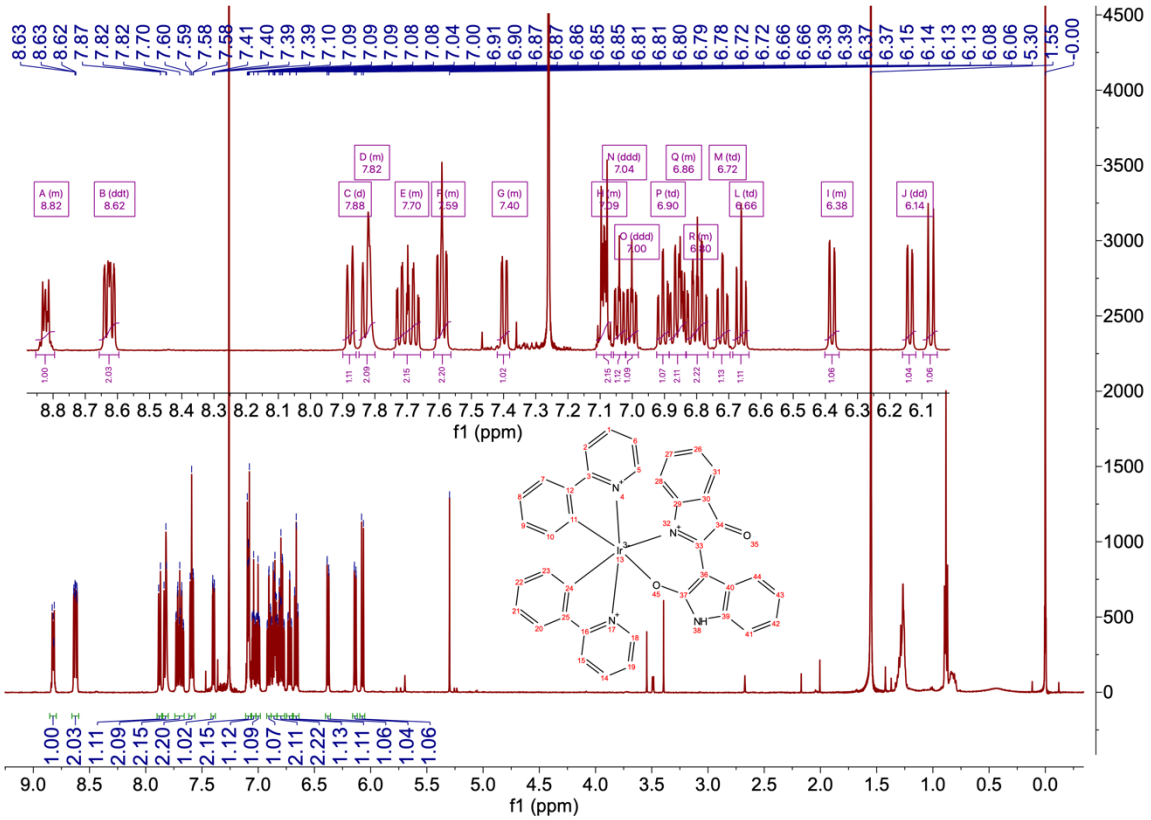


**Figure S2.** $^{1}$H-NMR spectrum of complex **1**.

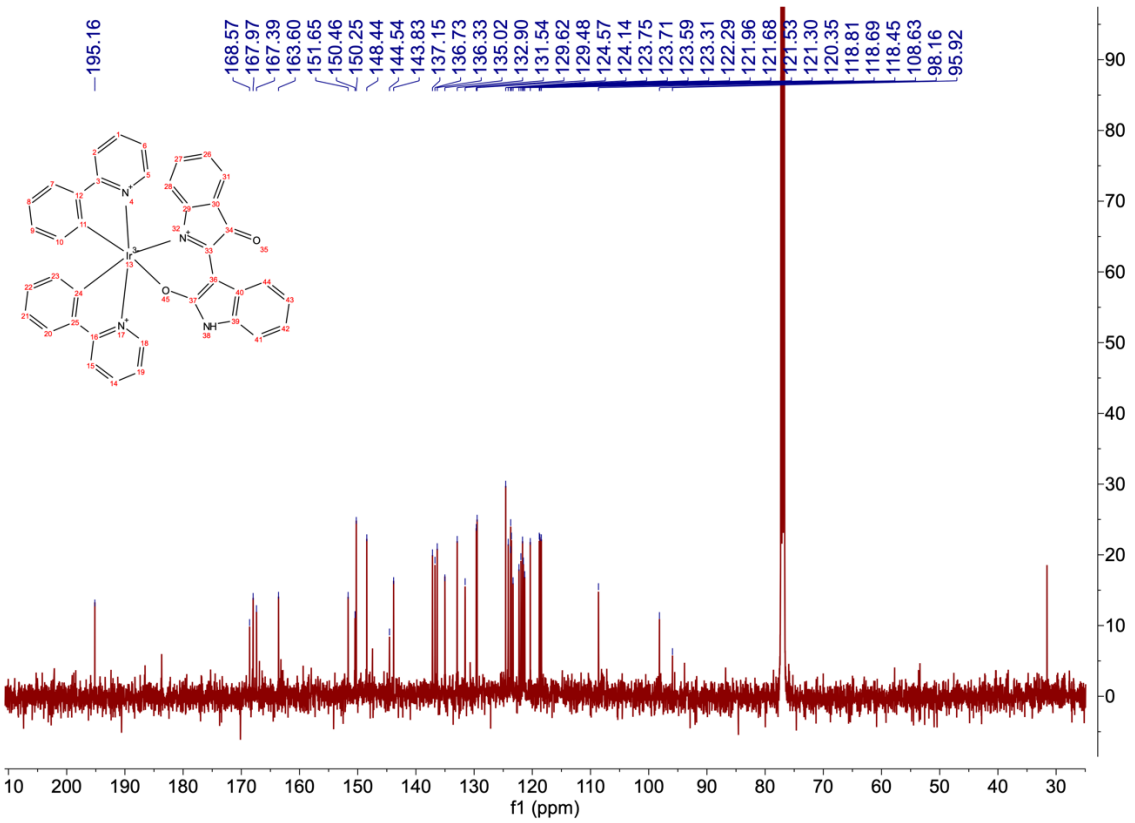


**Figure S3.** $^{13}$C-NMR spectrum of complex **1**.

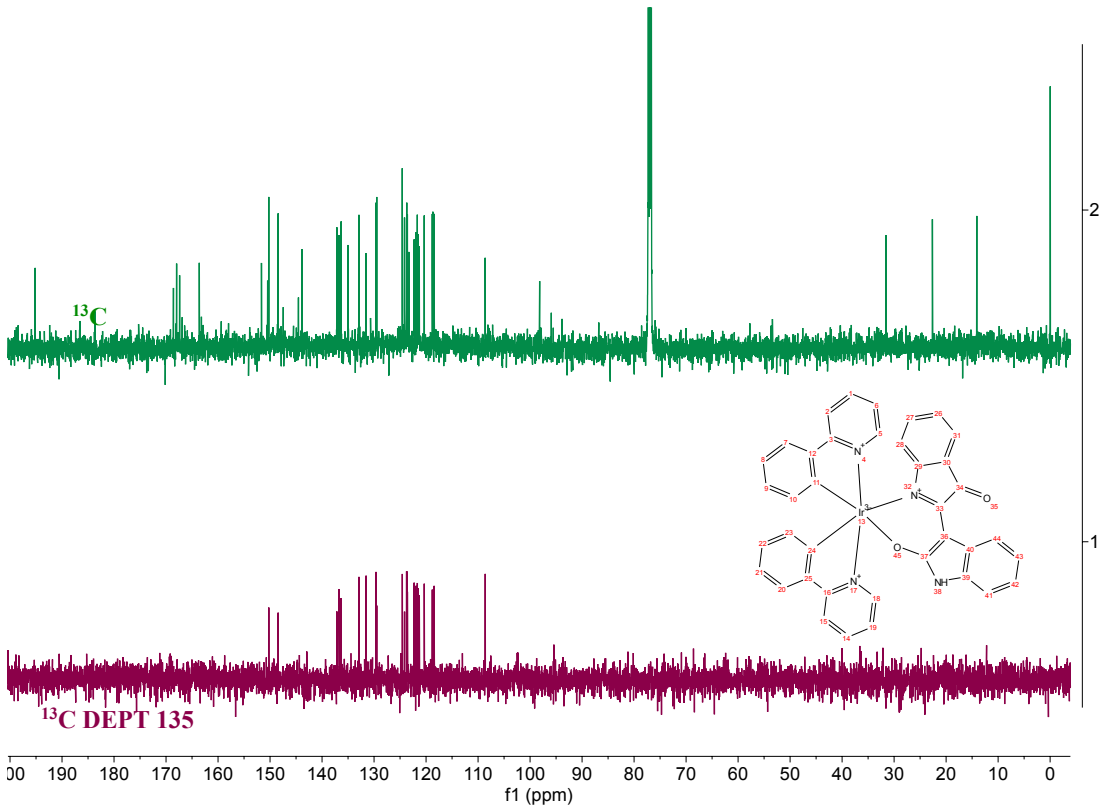


**Figure S4.** DEPT135 NMR spectrum of complex **1**.

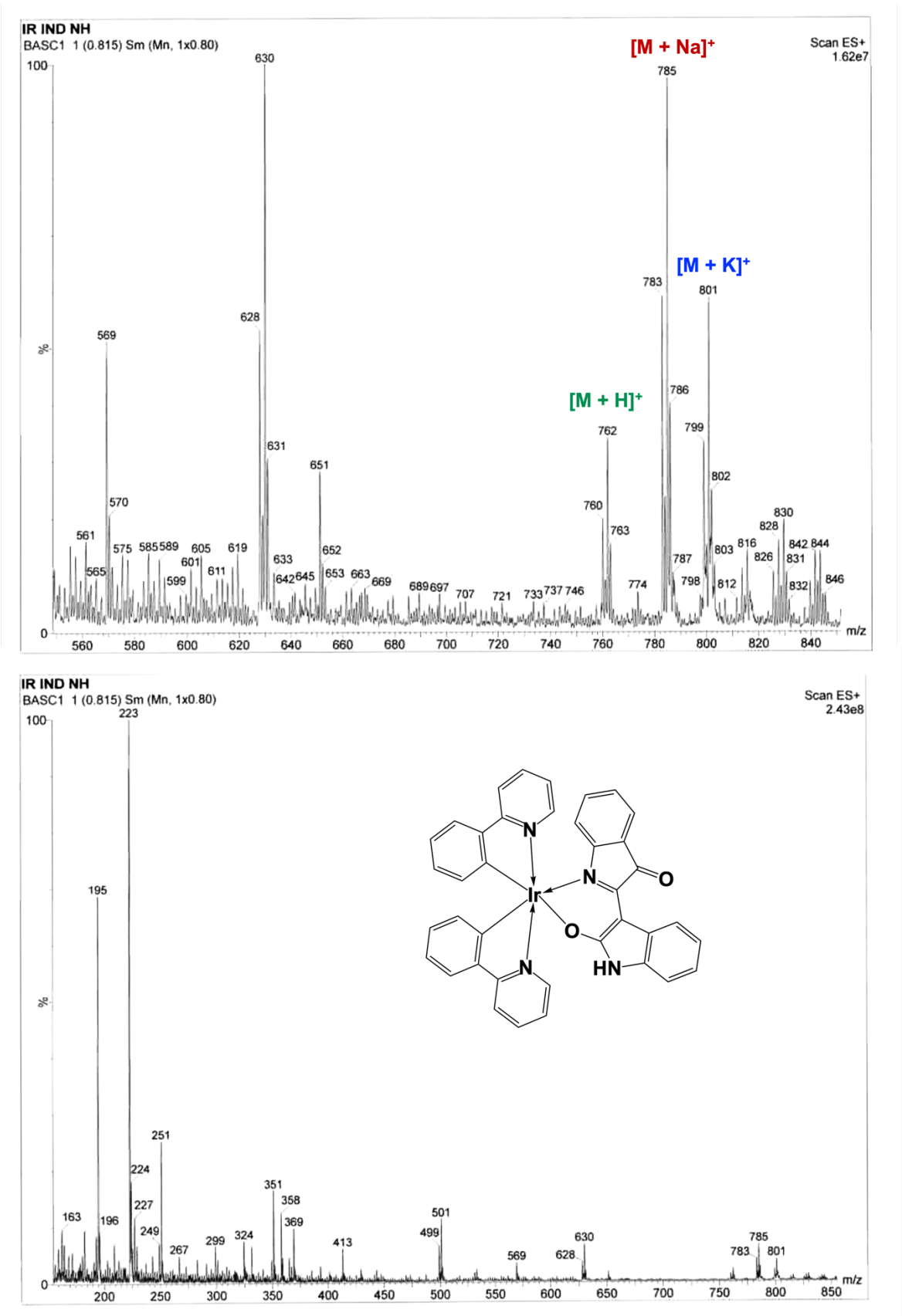


**Figure S5.** ESI$^+$ spectra of complex **1**.

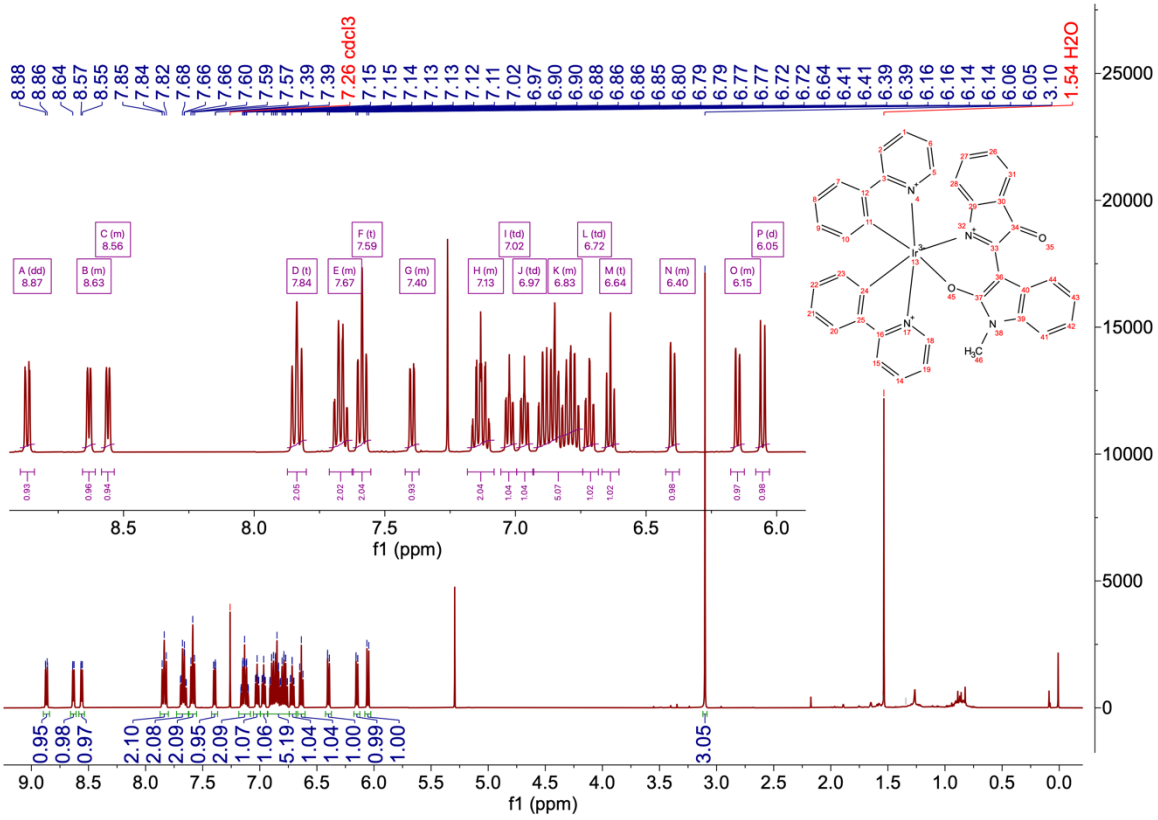


**Figure S6.** $^{1}$H-NMR spectrum of complex **2**.

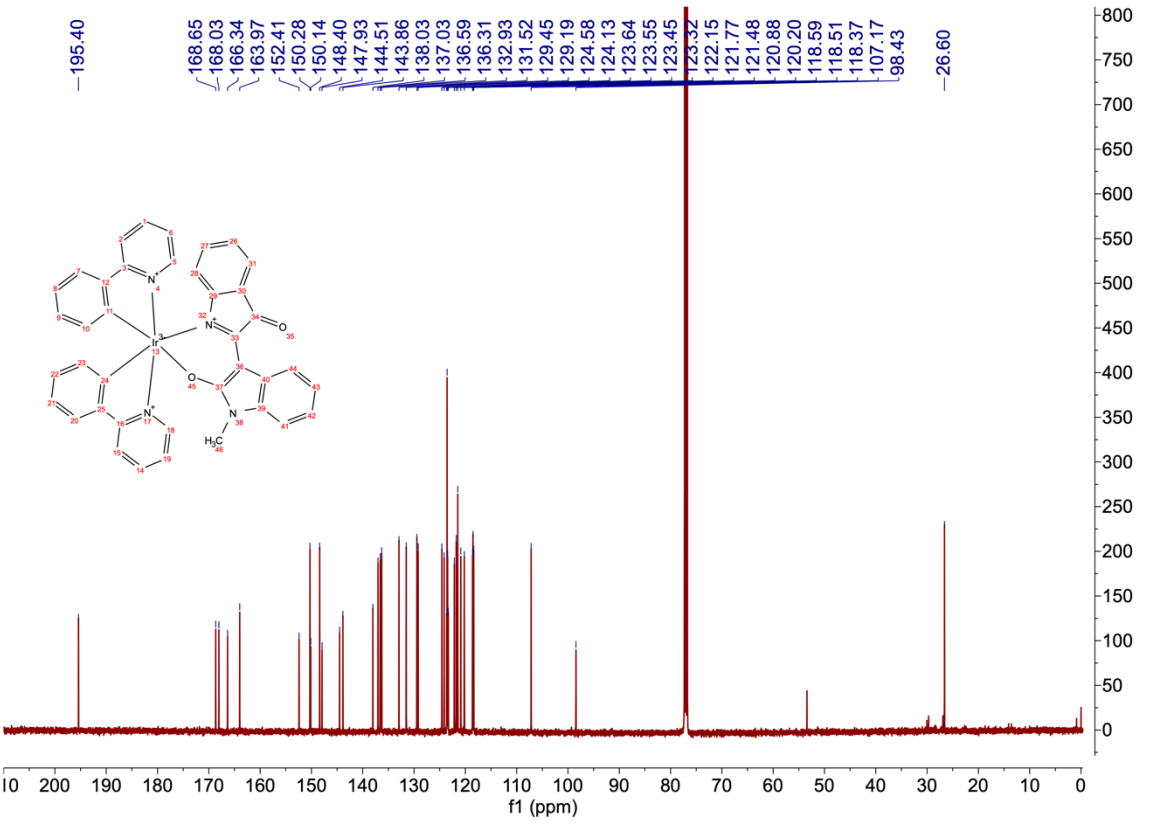


**Figure S7.** $^{13}$C-NMR spectrum of complex **2**.

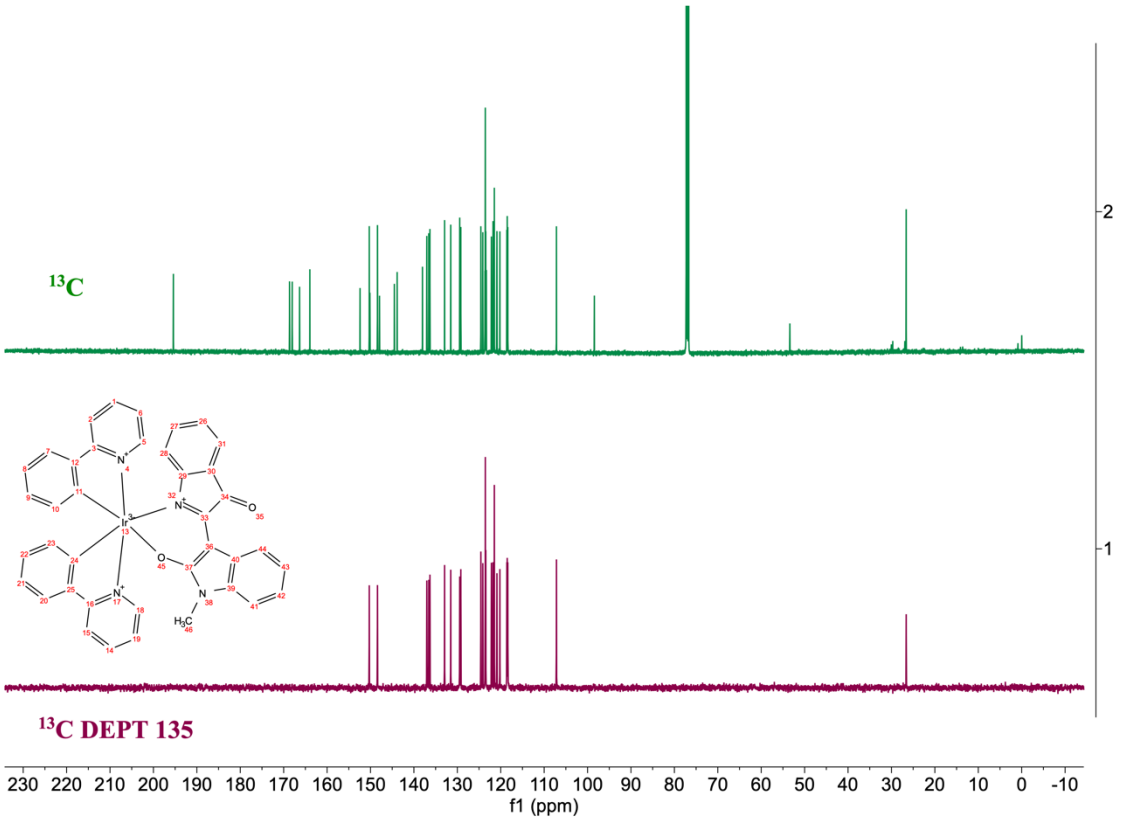


**Figure S8.** DEPT135 NMR spectrum of complex **2**.

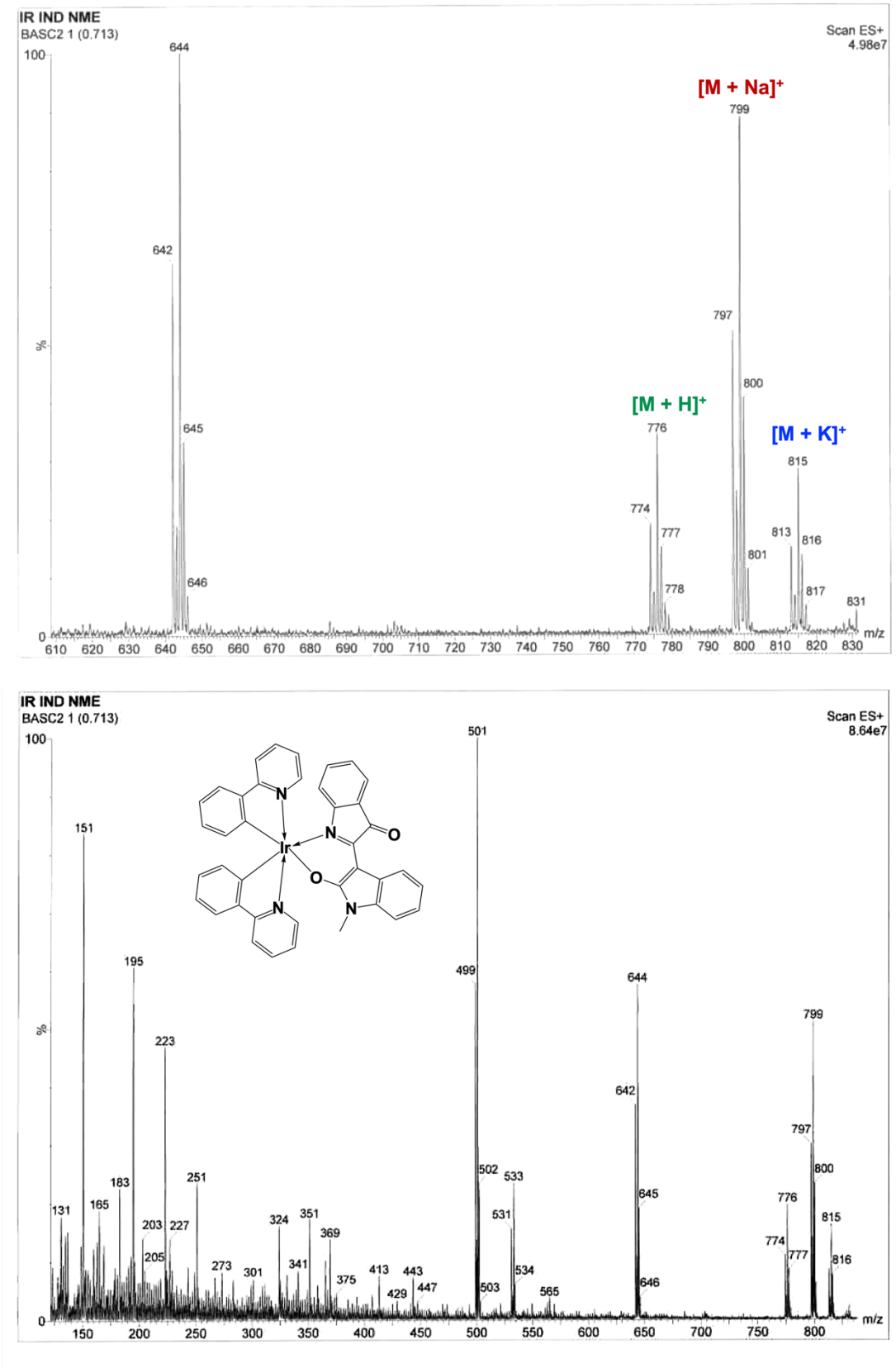


**Figure S9.** ESI$^+$ spectra of complex **2**.

## X-Ray data for Complex 2

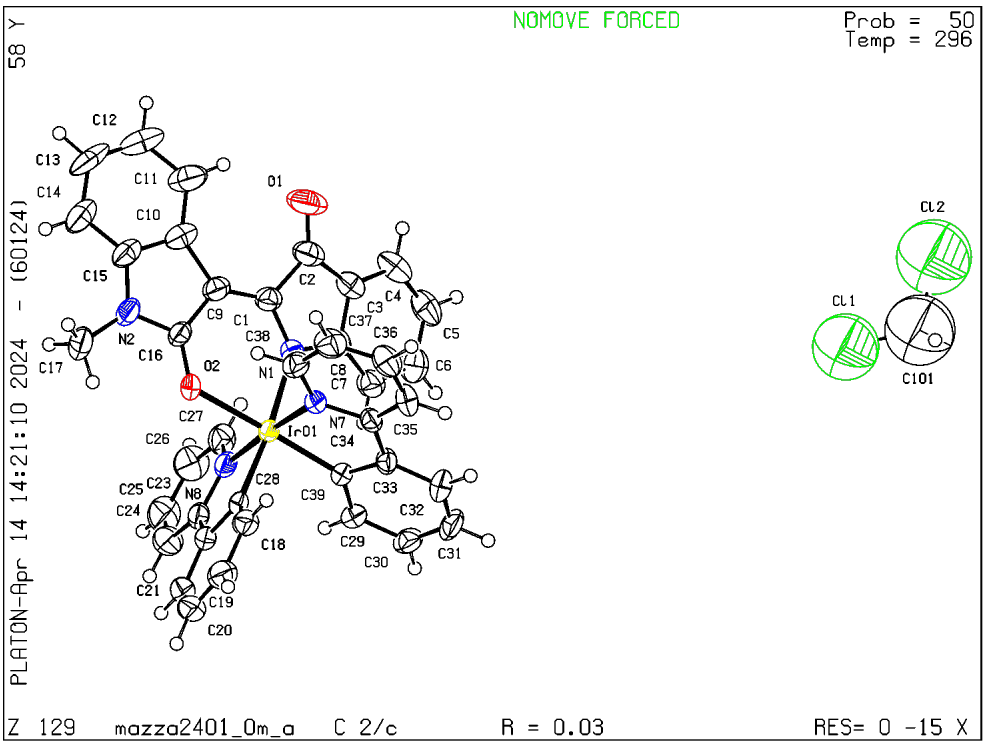


A specimen of $C_{39}H_{27}Cl_2IrN_4O_2$, approximate dimensions 0.100 mm x 0.100 mm x 0.300 mm, was used for the X-ray crystallographic analysis. The X-ray intensity data were measured (λ = 0.71073 Å). The total exposure time was 20.33 hours. The frames were integrated with the Bruker SAINT software package using a narrow-frame algorithm. The integration of the data using a monoclinic unit cell yielded a total of 40137 reflections to a maximum θ angle of 25.00° (0.84 Å resolution), of which 5529 were independent (average redundancy 7.259, completeness = 99.7%, $R_{int}$ = 5.09%, $R_{sig}$ = 2.74%) and 5107 (92.37%) were greater than $2\sigma(F^2)$. The final cell constants of a = 31.637(13) Å, b = 17.441(8) Å, c = 11.578(5) Å, β = 99.926(18)°, volume = 6293.(5) $Å^3$, are based upon the refinement of the XYZ-centroids of 9992 reflections above 20 σ(I) with 4.548° < 2θ < 60.64°. Data were corrected for absorption effects using the Multi-Scan method (SADABS). The ratio of minimum to maximum apparent transmission was 0.756. The calculated minimum and maximum transmission coefficients (based on crystal size) are 0.3480 and 0.6640.

The structure was solved and refined using the Bruker SHELXTL Software Package, using the space group C 1 2/c 1, with Z = 8 for the formula unit, $C_{39}H_{27}Cl_2IrN_4O_2$. The final anisotropic full-matrix least-squares refinement on $F^2$ with 424 variables converged at R1 = 3.08%, for the observed data and wR2 = 7.13% for all data. The goodness-of-fit was 2.154. The largest peak in the final difference electron density synthesis was 0.990 $e^-/Å^3$ and the largest hole was -1.201 $e^-/Å^3$ with an RMS deviation of 0.098 $e^-/Å^3$. On the basis of the final model, the calculated density was 1.787 $g/cm^3$ and F(000), 3328 $e^-$.

**Table S1.** Sample and crystal data for complex **2**.

| | | |
|---|---|---|
| Identification code | mazza2401 | |
| Chemical formula | $C_{39}H_{27}Cl_2IrN_4O_2$ | |
| Formula weight | 846.74 g/mol | |
| Temperature | 296(2) K | |
| Wavelength | 0.71073 Å | |
| Crystal size | 0.100 x 0.100 x 0.300 mm | |
| Crystal system | monoclinic | |
| Space group | C 1 2/c 1 | |
| Unit cell dimensions | a = 31.637(13) Å | α = 90° |
| | b = 17.441(8) Å | β = 99.926(18)° |
| | c = 11.578(5) Å | γ = 90° |
| Volume | 6293.(5) $Å^3$ | |
| Z | 8 | |
| Density (calculated) | 1.787 $g/cm^3$ | |
| Absorption coefficient | 4.458 $mm^{-1}$ | |
| F(000) | 3328 | |

**Table S2.** Data collection and structure refinement for complex **2**.

| | | |
|---|---|---|
| Theta range for data collection | 2.32 to 25.00° | |
| Index ranges | -37<=h<=37, -20<=k<=20, -13<=l<=13 | |
| Reflections collected | 40137 | |
| Independent reflections | 5529 [R(int) = 0.0509] | |
| Coverage of independent reflections | 99.7% | |
| Absorption correction | Multi-Scan | |
| Max. and min. transmission | 0.6640 and 0.3480 | |
| Structure solution technique | direct methods | |
| Structure solution program | SHELXT 2014/5 (Sheldrick, 2014) | |
| Refinement method | Full-matrix least-squares on $F^2$ | |
| Refinement program | SHELXL-2017/1 (Sheldrick, 2017) | |
| Function minimized | $\Sigma\, w(F_o^2 - F_c^2)^2$ | |
| Data / restraints / parameters | 5529 / 1 / 424 | |
| Goodness-of-fit on $F^2$ | 2.154 | |
| $\Delta/\sigma_{max}$ | 0.004 | |
| Final R indices | 5107 data; I>2σ(I) | R1 = 0.0308, wR2 = 0.0708 |
| | all data | R1 = 0.0335, wR2 = 0.0713 |
| Weighting scheme | $w=1/[\sigma^2(F_o^2)+0.6459P]$ where $P=(F_o^2+2F_c^2)/3$ | |
| Largest diff. peak and hole | 0.990 and -1.201 $eÅ^{-3}$ | |
| R.M.S. deviation from mean | 0.098 $eÅ^{-3}$ | |

**Table S3.** Atomic coordinates and equivalent isotropic atomic displacement parameters (Å$^2$) for complex **2**.

U(eq) is defined as one third of the trace of the orthogonalized $U_{ij}$ tensor.

| | x/a | y/b | z/c | U(eq) |
|---|---|---|---|---|
| Ir01 | 0.64590(2) | 0.30743(2) | 0.37152(2) | 0.02859(7) |
| O2 | 0.66949(11) | 0.19346(16) | 0.4154(3) | 0.0393(8) |
| N7 | 0.67804(11) | 0.3571(2) | 0.5201(3) | 0.0302(8) |
| N8 | 0.61395(13) | 0.2645(2) | 0.2182(3) | 0.0356(9) |
| N1 | 0.59667(12) | 0.2800(2) | 0.4723(3) | 0.0337(9) |
| C28 | 0.69116(15) | 0.3212(2) | 0.2717(4) | 0.0319(10) |
| N2 | 0.67273(14) | 0.0766(2) | 0.5031(3) | 0.0443(10) |
| C22 | 0.67863(18) | 0.2964(2) | 0.1545(4) | 0.0398(12) |
| C34 | 0.67236(14) | 0.4340(2) | 0.5309(4) | 0.0301(10) |
| C9 | 0.62540(16) | 0.1604(3) | 0.5617(4) | 0.0396(11) |
| C39 | 0.63068(14) | 0.4165(2) | 0.3368(4) | 0.0289(9) |
| C8 | 0.55915(15) | 0.3242(3) | 0.4788(4) | 0.0354(11) |
| C33 | 0.64604(14) | 0.4682(3) | 0.4279(4) | 0.0341(10) |
| C16 | 0.65646(15) | 0.1481(2) | 0.4867(4) | 0.0359(11) |
| C23 | 0.63557(17) | 0.2648(3) | 0.1264(4) | 0.0405(12) |
| C1 | 0.59868(16) | 0.2230(3) | 0.5525(4) | 0.0380(11) |
| C3 | 0.53906(17) | 0.3008(3) | 0.5701(4) | 0.0431(12) |
| C29 | 0.60755(15) | 0.4482(3) | 0.2340(4) | 0.0378(11) |
| C10 | 0.62490(17) | 0.0880(3) | 0.6273(4) | 0.0471(13) |
| C38 | 0.70239(16) | 0.3193(3) | 0.6083(4) | 0.0402(12) |
| O1 | 0.56092(18) | 0.2076(3) | 0.7185(4) | 0.0897(16) |
| C18 | 0.73211(15) | 0.3513(3) | 0.3021(4) | 0.0396(11) |
| C32 | 0.63586(16) | 0.5457(3) | 0.4185(5) | 0.0446(12) |
| C7 | 0.54093(16) | 0.3798(3) | 0.4033(4) | 0.0456(13) |
| C35 | 0.69093(15) | 0.4718(3) | 0.6312(4) | 0.0424(12) |
| C27 | 0.57453(17) | 0.2361(3) | 0.2033(5) | 0.0465(13) |
| C2 | 0.56438(18) | 0.2386(3) | 0.6273(4) | 0.0505(14) |
| C37 | 0.72075(17) | 0.3546(3) | 0.7096(4) | 0.0503(13) |
| C17 | 0.70578(19) | 0.0439(3) | 0.4464(5) | 0.0575(15) |
| C15 | 0.65334(18) | 0.0381(3) | 0.5843(4) | 0.0467(13) |
| C21 | 0.7065(2) | 0.3040(3) | 0.0747(5) | 0.0518(15) |
| C30 | 0.59784(16) | 0.5255(3) | 0.2244(4) | 0.0447(13) |
| C20 | 0.7461(2) | 0.3353(3) | 0.1076(5) | 0.0558(15) |
| C24 | 0.6164(2) | 0.2358(3) | 0.0197(5) | 0.0568(15) |
| C19 | 0.75919(18) | 0.3582(3) | 0.2211(5) | 0.0528(14) |
| C13 | 0.6373(2) | 0.9368(4) | 0.7031(6) | 0.075(2) |
| C31 | 0.61121(17) | 0.5737(3) | 0.3177(5) | 0.0493(13) |
| C4 | 0.50169(18) | 0.3348(4) | 0.5899(5) | 0.0586(15) |
| C36 | 0.71436(17) | 0.4312(3) | 0.7209(4) | 0.0499(14) |
| C26 | 0.5542(2) | 0.2067(3) | 0.0983(5) | 0.0647(17) |
| C6 | 0.50309(17) | 0.4134(3) | 0.4246(5) | 0.0548(14) |
| C25 | 0.5758(2) | 0.2063(3) | 0.0055(5) | 0.0685(19) |
| C14 | 0.6594(2) | 0.9636(3) | 0.6204(5) | 0.0624(17) |
| C11 | 0.6039(2) | 0.0592(4) | 0.7120(5) | 0.0711(19) |
| C5 | 0.48374(19) | 0.3922(4) | 0.5170(5) | 0.0632(17) |
| C12 | 0.6103(2) | 0.9844(4) | 0.7473(6) | 0.081(2) |
| C100 | 0.5121(4) | 0.0198(7) | 0.9264(10) | 0.171(5) |
| C101 | 0.5245(3) | 0.9471(6) | 0.9229(8) | 0.120(3) |

**Table S4.** Bond lengths (Å) for complex **2**.

| | | | |
|---|---|---|---|
| Ir01-C39 | 1.986(4) | Ir01-C28 | 2.003(4) |
| Ir01-N8 | 2.028(4) | Ir01-N7 | 2.034(4) |
| Ir01-N1 | 2.154(4) | Ir01-O2 | 2.153(3) |
| O2-C16 | 1.263(5) | N7-C38 | 1.342(6) |
| N7-C34 | 1.362(5) | N8-C27 | 1.325(6) |
| N8-C23 | 1.360(6) | N1-C1 | 1.355(6) |
| N1-C8 | 1.428(6) | C28-C18 | 1.386(6) |
| C28-C22 | 1.416(6) | N2-C16 | 1.351(6) |
| N2-C15 | 1.382(6) | N2-C17 | 1.443(6) |
| C22-C21 | 1.389(7) | C22-C23 | 1.453(7) |
| C34-C35 | 1.376(6) | C34-C33 | 1.459(6) |
| C9-C1 | 1.374(7) | C9-C16 | 1.435(6) |
| C9-C10 | 1.474(6) | C39-C29 | 1.399(6) |
| C39-C33 | 1.409(6) | C8-C7 | 1.366(7) |
| C8-C3 | 1.386(7) | C33-C32 | 1.390(6) |
| C23-C24 | 1.375(7) | C1-C2 | 1.525(7) |
| C3-C4 | 1.377(7) | C3-C2 | 1.440(7) |
| C29-C30 | 1.384(6) | C29-H29 | 0.93 |
| C10-C11 | 1.372(7) | C10-C15 | 1.403(7) |
| C38-C37 | 1.363(7) | C38-H38 | 0.93 |
| O1-C2 | 1.208(6) | C18-C19 | 1.380(7) |
| C18-H18 | 0.93 | C32-C31 | 1.377(7) |
| C32-H32 | 0.93 | C7-C6 | 1.392(7) |
| C7-H7 | 0.93 | C35-C36 | 1.365(7) |
| C35-H35 | 0.93 | C27-C26 | 1.373(7) |
| C27-H27 | 0.93 | C37-C36 | 1.361(7) |
| C37-H37 | 0.93 | C17-H17A | 0.96 |
| C17-H17B | 0.96 | C17-H17C | 0.96 |
| C15-C14 | 1.368(7) | C21-C20 | 1.359(8) |
| C21-H21 | 0.93 | C30-C31 | 1.377(7) |
| C30-H30 | 0.93 | C20-C19 | 1.368(8) |
| C20-H20 | 0.93 | C24-C25 | 1.366(8) |
| C24-H24 | 0.93 | C19-H19 | 0.93 |
| C13-C12 | 1.352(9) | C13-C14 | 1.364(8) |
| C13-H13 | 0.93 | C31-H31 | 0.93 |
| C4-C5 | 1.368(8) | C4-H4 | 0.93 |
| C36-H36 | 0.93 | C26-C25 | 1.371(9) |
| C26-H26 | 0.93 | C6-C5 | 1.372(8) |
| C6-H6 | 0.93 | C25-H25 | 0.93 |
| C14-H14 | 0.93 | C11-C12 | 1.373(8) |
| C11-H11 | 0.93 | C5-H5 | 0.93 |
| C12-H12 | 0.93 | C100-C101 | 1.330(12) |

**Table S5.** Bond angles (°) for complex **2**.

| | | | |
|---|---|---|---|
| C39-Ir01-C28 | 86.61(16) | C39-Ir01-N8 | 96.28(16) |
| C28-Ir01-N8 | 80.65(18) | C39-Ir01-N7 | 80.31(16) |
| C28-Ir01-N7 | 97.68(17) | N8-Ir01-N7 | 176.31(14) |
| C39-Ir01-N1 | 98.58(15) | C28-Ir01-N1 | 173.84(15) |
| N8-Ir01-N1 | 95.42(15) | N7-Ir01-N1 | 86.52(14) |
| C39-Ir01-O2 | 173.72(15) | C28-Ir01-O2 | 89.63(14) |
| N8-Ir01-O2 | 88.05(14) | N7-Ir01-O2 | 95.24(13) |
| N1-Ir01-O2 | 85.48(13) | C16-O2-Ir01 | 126.4(3) |

| | | | |
|---|---|---|---|
| C38-N7-C34 | 118.8(4) | C38-N7-Ir01 | 124.9(3) |
| C34-N7-Ir01 | 116.3(3) | C27-N8-C23 | 119.2(4) |
| C27-N8-Ir01 | 124.6(3) | C23-N8-Ir01 | 116.2(3) |
| C1-N1-C8 | 107.5(4) | C1-N1-Ir01 | 125.5(3) |
| C8-N1-Ir01 | 126.5(3) | C18-C28-C22 | 117.0(4) |
| C18-C28-Ir01 | 129.0(4) | C22-C28-Ir01 | 114.0(4) |
| C16-N2-C15 | 109.9(4) | C16-N2-C17 | 126.1(4) |
| C15-N2-C17 | 124.0(4) | C21-C22-C28 | 120.2(5) |
| C21-C22-C23 | 124.5(5) | C28-C22-C23 | 115.3(4) |
| N7-C34-C35 | 120.4(4) | N7-C34-C33 | 113.1(4) |
| C35-C34-C33 | 126.5(4) | C1-C9-C16 | 123.3(4) |
| C1-C9-C10 | 131.2(5) | C16-C9-C10 | 104.6(4) |
| C29-C39-C33 | 116.5(4) | C29-C39-Ir01 | 128.6(3) |
| C33-C39-Ir01 | 114.9(3) | C7-C8-C3 | 119.9(5) |
| C7-C8-N1 | 127.8(4) | C3-C8-N1 | 112.1(4) |
| C32-C33-C39 | 121.3(4) | C32-C33-C34 | 123.6(4) |
| C39-C33-C34 | 115.1(4) | O2-C16-N2 | 120.7(4) |
| O2-C16-C9 | 129.5(4) | N2-C16-C9 | 109.7(4) |
| N8-C23-C24 | 119.9(5) | N8-C23-C22 | 113.9(4) |
| C24-C23-C22 | 126.3(5) | N1-C1-C9 | 126.3(4) |
| N1-C1-C2 | 107.8(4) | C9-C1-C2 | 125.9(4) |
| C8-C3-C4 | 121.3(5) | C8-C3-C2 | 106.3(4) |
| C4-C3-C2 | 132.3(5) | C30-C29-C39 | 122.0(5) |
| C30-C29-H29 | 119.0 | C39-C29-H29 | 119.0 |
| C11-C10-C15 | 116.4(5) | C11-C10-C9 | 137.0(6) |
| C15-C10-C9 | 106.5(4) | N7-C38-C37 | 122.4(5) |
| N7-C38-H38 | 118.8 | C37-C38-H38 | 118.8 |
| C19-C18-C28 | 121.6(5) | C19-C18-H18 | 119.2 |
| C28-C18-H18 | 119.2 | C31-C32-C33 | 120.1(5) |
| C31-C32-H32 | 120.0 | C33-C32-H32 | 120.0 |
| C8-C7-C6 | 117.8(5) | C8-C7-H7 | 121.1 |
| C6-C7-H7 | 121.1 | C36-C35-C34 | 119.4(5) |
| C36-C35-H35 | 120.3 | C34-C35-H35 | 120.3 |
| N8-C27-C26 | 122.8(5) | N8-C27-H27 | 118.6 |
| C26-C27-H27 | 118.6 | O1-C2-C3 | 127.7(5) |
| O1-C2-C1 | 126.7(5) | C3-C2-C1 | 105.5(4) |
| C38-C37-C36 | 118.6(5) | C38-C37-H37 | 120.7 |
| C36-C37-H37 | 120.7 | N2-C17-H17A | 109.5 |
| N2-C17-H17B | 109.5 | H17A-C17-H17B | 109.5 |
| N2-C17-H17C | 109.5 | H17A-C17-H17C | 109.5 |
| H17B-C17-H17C | 109.5 | C14-C15-N2 | 127.8(6) |
| C14-C15-C10 | 123.1(5) | N2-C15-C10 | 109.1(4) |
| C20-C21-C22 | 120.9(5) | C20-C21-H21 | 119.6 |
| C22-C21-H21 | 119.6 | C29-C30-C31 | 119.9(5) |
| C29-C30-H30 | 120.1 | C31-C30-H30 | 120.1 |
| C21-C20-C19 | 119.8(5) | C21-C20-H20 | 120.1 |
| C19-C20-H20 | 120.1 | C25-C24-C23 | 120.4(6) |
| C25-C24-H24 | 119.8 | C23-C24-H24 | 119.8 |
| C20-C19-C18 | 120.5(5) | C20-C19-H19 | 119.8 |
| C18-C19-H19 | 119.8 | C12-C13-C14 | 119.3(6) |
| C12-C13-H13 | 120.4 | C14-C13-H13 | 120.4 |
| C32-C31-C30 | 120.1(5) | C32-C31-H31 | 120.0 |
| C30-C31-H31 | 120.0 | C5-C4-C3 | 119.3(5) |
| C5-C4-H4 | 120.4 | C3-C4-H4 | 120.4 |
| C35-C36-C37 | 120.4(5) | C35-C36-H36 | 119.8 |

| | | | |
|---|---|---|---|
| C37-C36-H36 | 119.8 | C25-C26-C27 | 118.3(6) |
| C25-C26-H26 | 120.9 | C27-C26-H26 | 120.9 |
| C5-C6-C7 | 122.5(6) | C5-C6-H6 | 118.7 |
| C7-C6-H6 | 118.7 | C26-C25-C24 | 119.4(6) |
| C26-C25-H25 | 120.3 | C24-C25-H25 | 120.3 |
| C13-C14-C15 | 118.6(6) | C13-C14-H14 | 120.7 |
| C15-C14-H14 | 120.7 | C10-C11-C12 | 119.7(7) |
| C10-C11-H11 | 120.1 | C12-C11-H11 | 120.1 |
| C4-C5-C6 | 119.0(5) | C4-C5-H5 | 120.5 |
| C6-C5-H5 | 120.5 | C13-C12-C11 | 122.9(6) |
| C13-C12-H12 | 118.6 | C11-C12-H12 | 118.6 |

**Table S6.** Torsion angles (°) for complex **2**.

| | | | |
|---|---|---|---|
| C18-C28-C22-C21 | -1.3(6) | Ir01-C28-C22-C21 | 178.7(3) |
| C18-C28-C22-C23 | 179.6(4) | Ir01-C28-C22-C23 | -0.4(5) |
| C38-N7-C34-C35 | -0.7(6) | Ir01-N7-C34-C35 | 176.4(3) |
| C38-N7-C34-C33 | 178.7(4) | Ir01-N7-C34-C33 | -4.1(5) |
| C1-N1-C8-C7 | -169.5(5) | Ir01-N1-C8-C7 | 18.3(7) |
| C1-N1-C8-C3 | 5.8(5) | Ir01-N1-C8-C3 | -166.4(3) |
| C29-C39-C33-C32 | 4.6(7) | Ir01-C39-C33-C32 | -176.4(4) |
| C29-C39-C33-C34 | -176.2(4) | Ir01-C39-C33-C34 | 2.8(5) |
| N7-C34-C33-C32 | -180.0(4) | C35-C34-C33-C32 | -0.6(7) |
| N7-C34-C33-C39 | 0.9(6) | C35-C34-C33-C39 | -179.7(4) |
| Ir01-O2-C16-N2 | 177.2(3) | Ir01-O2-C16-C9 | -4.2(7) |
| C15-N2-C16-O2 | -179.7(4) | C17-N2-C16-O2 | 1.0(8) |
| C15-N2-C16-C9 | 1.5(6) | C17-N2-C16-C9 | -177.8(5) |
| C1-C9-C16-O2 | 11.5(8) | C10-C9-C16-O2 | -178.0(5) |
| C1-C9-C16-N2 | -169.8(5) | C10-C9-C16-N2 | 0.7(5) |
| C27-N8-C23-C24 | 0.1(7) | Ir01-N8-C23-C24 | 179.2(4) |
| C27-N8-C23-C22 | -179.1(4) | Ir01-N8-C23-C22 | 0.0(5) |
| C21-C22-C23-N8 | -178.8(4) | C28-C22-C23-N8 | 0.3(6) |
| C21-C22-C23-C24 | 2.1(8) | C28-C22-C23-C24 | -178.8(5) |
| C8-N1-C1-C9 | 168.3(5) | Ir01-N1-C1-C9 | -19.5(7) |
| C8-N1-C1-C2 | -8.9(5) | Ir01-N1-C1-C2 | 163.4(3) |
| C16-C9-C1-N1 | 1.8(8) | C10-C9-C1-N1 | -165.9(5) |
| C16-C9-C1-C2 | 178.5(5) | C10-C9-C1-C2 | 10.8(9) |
| C7-C8-C3-C4 | -2.8(8) | N1-C8-C3-C4 | -178.5(5) |
| C7-C8-C3-C2 | 175.9(5) | N1-C8-C3-C2 | 0.3(6) |
| C33-C39-C29-C30 | -4.0(7) | Ir01-C39-C29-C30 | 177.2(4) |
| C1-C9-C10-C11 | -11.0(11) | C16-C9-C10-C11 | 179.6(6) |
| C1-C9-C10-C15 | 166.9(5) | C16-C9-C10-C15 | -2.6(5) |
| C34-N7-C38-C37 | 1.7(7) | Ir01-N7-C38-C37 | -175.2(4) |
| C22-C28-C18-C19 | 1.3(7) | Ir01-C28-C18-C19 | -178.6(4) |
| C39-C33-C32-C31 | -1.6(7) | C34-C33-C32-C31 | 179.3(4) |
| C3-C8-C7-C6 | 2.5(7) | N1-C8-C7-C6 | 177.4(5) |
| N7-C34-C35-C36 | -1.4(7) | C33-C34-C35-C36 | 179.2(4) |
| C23-N8-C27-C26 | -0.2(8) | Ir01-N8-C27-C26 | -179.2(4) |
| C8-C3-C2-O1 | 170.9(6) | C4-C3-C2-O1 | -10.5(11) |
| C8-C3-C2-C1 | -5.5(6) | C4-C3-C2-C1 | 173.1(6) |
| N1-C1-C2-O1 | -167.3(6) | C9-C1-C2-O1 | 15.5(9) |
| N1-C1-C2-C3 | 9.1(5) | C9-C1-C2-C3 | -168.1(5) |
| N7-C38-C37-C36 | -0.6(8) | C16-N2-C15-C14 | 176.6(5) |
| C17-N2-C15-C14 | -4.1(9) | C16-N2-C15-C10 | -3.2(6) |
| C17-N2-C15-C10 | 176.1(5) | C11-C10-C15-C14 | 2.1(8) |

| | | | |
|---|---|---|---|
| C9-C10-C15-C14 | -176.3(5) | C11-C10-C15-N2 | -178.1(5) |
| C9-C10-C15-N2 | 3.5(6) | C28-C22-C21-C20 | -0.1(7) |
| C23-C22-C21-C20 | 179.0(5) | C39-C29-C30-C31 | 0.3(7) |
| C22-C21-C20-C19 | 1.4(8) | N8-C23-C24-C25 | -0.4(8) |
| C22-C23-C24-C25 | 178.7(5) | C21-C20-C19-C18 | -1.3(8) |
| C28-C18-C19-C20 | -0.1(8) | C33-C32-C31-C30 | -2.3(8) |
| C29-C30-C31-C32 | 2.9(8) | C8-C3-C4-C5 | 0.9(9) |
| C2-C3-C4-C5 | -177.5(6) | C34-C35-C36-C37 | 2.6(8) |
| C38-C37-C36-C35 | -1.6(8) | N8-C27-C26-C25 | 0.6(9) |
| C8-C7-C6-C5 | -0.4(8) | C27-C26-C25-C24 | -0.9(9) |
| C23-C24-C25-C26 | 0.8(9) | C12-C13-C14-C15 | -0.4(10) |
| N2-C15-C14-C13 | 179.3(5) | C10-C15-C14-C13 | -0.9(9) |
| C15-C10-C11-C12 | -2.0(9) | C9-C10-C11-C12 | 175.8(6) |
| C3-C4-C5-C6 | 1.1(9) | C7-C6-C5-C4 | -1.4(9) |
| C14-C13-C12-C11 | 0.5(12) | C10-C11-C12-C13 | 0.7(11) |

**Table S7.** Anisotropic atomic displacement parameters ($Å^2$) for complex **2**.

The anisotropic atomic displacement factor exponent takes the form: $-2\pi^2[ h^2 a^{*2} U_{11} + ... + 2 h k a^* b^* U_{12} ]$

| | $U_{11}$ | $U_{22}$ | $U_{33}$ | $U_{23}$ | $U_{13}$ | $U_{12}$ |
|---|---|---|---|---|---|---|
| Ir01 | 0.03788(11) | 0.02195(10) | 0.02610(10) | -0.00035(7) | 0.00598(7) | 0.00110(8) |
| O2 | 0.056(2) | 0.0252(17) | 0.0397(19) | 0.0003(14) | 0.0157(17) | 0.0094(15) |
| N7 | 0.035(2) | 0.029(2) | 0.0267(19) | -0.0004(16) | 0.0068(17) | 0.0017(16) |
| N8 | 0.050(3) | 0.023(2) | 0.032(2) | -0.0017(16) | 0.0032(19) | -0.0009(18) |
| N1 | 0.038(2) | 0.032(2) | 0.032(2) | -0.0021(17) | 0.0087(18) | -0.0017(17) |
| C28 | 0.040(3) | 0.023(2) | 0.034(3) | 0.0040(19) | 0.011(2) | 0.0096(19) |
| N2 | 0.061(3) | 0.027(2) | 0.044(2) | 0.0049(19) | 0.006(2) | 0.006(2) |
| C22 | 0.064(3) | 0.026(2) | 0.032(3) | 0.002(2) | 0.015(2) | 0.008(2) |
| C34 | 0.030(2) | 0.031(2) | 0.032(2) | -0.005(2) | 0.0104(19) | 0.0016(19) |
| C9 | 0.049(3) | 0.034(3) | 0.035(3) | 0.006(2) | 0.005(2) | -0.002(2) |
| C39 | 0.032(2) | 0.024(2) | 0.031(2) | 0.0012(19) | 0.0069(19) | 0.0014(19) |
| C8 | 0.036(3) | 0.035(3) | 0.035(3) | -0.011(2) | 0.007(2) | -0.003(2) |
| C33 | 0.036(3) | 0.029(2) | 0.039(3) | -0.002(2) | 0.011(2) | 0.007(2) |
| C16 | 0.049(3) | 0.024(2) | 0.034(3) | 0.001(2) | 0.005(2) | -0.003(2) |
| C23 | 0.064(3) | 0.025(2) | 0.033(3) | -0.002(2) | 0.007(2) | 0.004(2) |
| C1 | 0.043(3) | 0.040(3) | 0.031(3) | -0.001(2) | 0.007(2) | -0.007(2) |
| C3 | 0.045(3) | 0.051(3) | 0.035(3) | -0.004(2) | 0.010(2) | 0.001(2) |
| C29 | 0.045(3) | 0.033(3) | 0.036(3) | 0.004(2) | 0.009(2) | 0.002(2) |
| C10 | 0.053(3) | 0.043(3) | 0.043(3) | 0.012(2) | 0.001(3) | -0.010(3) |
| C38 | 0.049(3) | 0.035(3) | 0.036(3) | 0.005(2) | 0.005(2) | 0.005(2) |
| O1 | 0.119(4) | 0.103(4) | 0.059(3) | 0.033(3) | 0.052(3) | 0.034(3) |
| C18 | 0.041(3) | 0.038(3) | 0.042(3) | 0.004(2) | 0.011(2) | 0.003(2) |
| C32 | 0.049(3) | 0.026(2) | 0.058(3) | -0.006(2) | 0.007(3) | 0.002(2) |
| C7 | 0.039(3) | 0.052(3) | 0.046(3) | 0.001(3) | 0.011(2) | 0.009(2) |
| C35 | 0.039(3) | 0.042(3) | 0.047(3) | -0.016(2) | 0.009(2) | 0.002(2) |
| C27 | 0.054(3) | 0.039(3) | 0.044(3) | -0.008(2) | 0.002(3) | -0.006(3) |
| C2 | 0.058(4) | 0.061(4) | 0.035(3) | 0.002(3) | 0.016(3) | -0.005(3) |
| C37 | 0.052(3) | 0.059(4) | 0.035(3) | 0.002(3) | -0.004(2) | 0.001(3) |
| C17 | 0.079(4) | 0.034(3) | 0.061(4) | 0.002(3) | 0.014(3) | 0.014(3) |
| C15 | 0.059(3) | 0.032(3) | 0.044(3) | 0.006(2) | -0.004(3) | -0.009(2) |
| C21 | 0.079(4) | 0.041(3) | 0.040(3) | 0.001(2) | 0.023(3) | 0.012(3) |
| C30 | 0.045(3) | 0.042(3) | 0.047(3) | 0.015(2) | 0.010(2) | 0.006(2) |
| C20 | 0.070(4) | 0.049(3) | 0.057(4) | 0.010(3) | 0.035(3) | 0.014(3) |
| C24 | 0.085(5) | 0.049(3) | 0.035(3) | -0.005(3) | 0.006(3) | -0.005(3) |

| | $U_{11}$ | $U_{22}$ | $U_{33}$ | $U_{23}$ | $U_{13}$ | $U_{12}$ |
|---|---|---|---|---|---|---|
| C19 | 0.052(3) | 0.047(3) | 0.063(4) | 0.007(3) | 0.020(3) | 0.005(3) |
| C13 | 0.102(6) | 0.040(4) | 0.078(5) | 0.031(3) | -0.003(4) | -0.014(4) |
| C31 | 0.056(3) | 0.025(3) | 0.068(4) | 0.008(3) | 0.014(3) | 0.012(2) |
| C4 | 0.053(4) | 0.082(4) | 0.045(3) | -0.010(3) | 0.019(3) | 0.002(3) |
| C36 | 0.053(3) | 0.061(4) | 0.034(3) | -0.016(3) | 0.002(2) | -0.002(3) |
| C26 | 0.071(4) | 0.064(4) | 0.054(4) | -0.009(3) | -0.003(3) | -0.020(3) |
| C6 | 0.049(3) | 0.053(3) | 0.062(4) | 0.001(3) | 0.007(3) | 0.011(3) |
| C25 | 0.099(6) | 0.059(4) | 0.041(3) | -0.012(3) | -0.009(4) | -0.007(4) |
| C14 | 0.085(5) | 0.030(3) | 0.068(4) | 0.007(3) | 0.000(3) | -0.002(3) |
| C11 | 0.077(5) | 0.071(5) | 0.068(4) | 0.031(3) | 0.021(4) | -0.004(3) |
| C5 | 0.049(4) | 0.084(5) | 0.059(4) | -0.014(3) | 0.018(3) | 0.014(3) |
| C12 | 0.091(5) | 0.071(5) | 0.082(5) | 0.045(4) | 0.014(4) | -0.013(4) |

**Table S8.** Hydrogen atomic coordinates and isotropic atomic displacement parameters ($Å^2$) for complex **2**.

| | x/a | y/b | z/c | U(eq) |
|---|---|---|---|---|
| H29 | 0.5984 | 0.4163 | 0.1702 | 0.045 |
| H38 | 0.7069 | 0.2670 | 0.6000 | 0.048 |
| H18 | 0.7416 | 0.3672 | 0.3789 | 0.048 |
| H32 | 0.6457 | 0.5787 | 0.4804 | 0.054 |
| H7 | 0.5534 | 0.3949 | 0.3398 | 0.055 |
| H35 | 0.6876 | 0.5245 | 0.6378 | 0.051 |
| H27 | 0.5601 | 0.2360 | 0.2668 | 0.056 |
| H37 | 0.7373 | 0.3269 | 0.7697 | 0.06 |
| H17A | 0.7154 | 0.0817 | 0.3963 | 0.086 |
| H17B | 0.6945 | 0.0004 | 0.4005 | 0.086 |
| H17C | 0.7295 | 0.0281 | 0.5048 | 0.086 |
| H21 | 0.6980 | 0.2874 | -0.0021 | 0.062 |
| H30 | 0.5823 | 0.5449 | 0.1550 | 0.054 |
| H20 | 0.7643 | 0.3411 | 0.0530 | 0.067 |
| H24 | 0.6312 | 0.2362 | -0.0432 | 0.068 |
| H19 | 0.7865 | 0.3787 | 0.2439 | 0.063 |
| H13 | 0.6406 | -0.1137 | 0.7289 | 0.09 |
| H31 | 0.6036 | 0.6253 | 0.3126 | 0.059 |
| H4 | 0.4888 | 0.3190 | 0.6523 | 0.07 |
| H36 | 0.7260 | 0.4561 | 0.7902 | 0.06 |
| H26 | 0.5264 | 0.1876 | 0.0904 | 0.078 |
| H6 | 0.4904 | 0.4516 | 0.3742 | 0.066 |
| H25 | 0.5630 | 0.1862 | -0.0664 | 0.082 |
| H14 | 0.6783 | -0.0680 | 0.5892 | 0.075 |
| H11 | 0.5853 | 0.0903 | 0.7453 | 0.085 |
| H5 | 0.4588 | 0.4165 | 0.5299 | 0.076 |
| H12 | 0.5956 | -0.0344 | 0.8042 | 0.098 |

Singly oxidised radicals

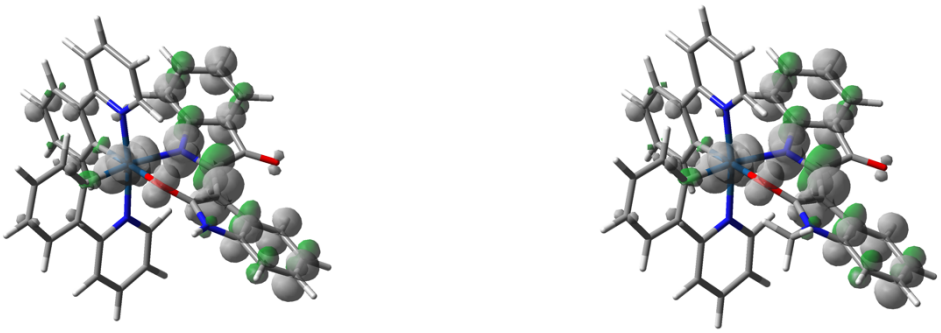

**1** **2**

Singly reduced radicals

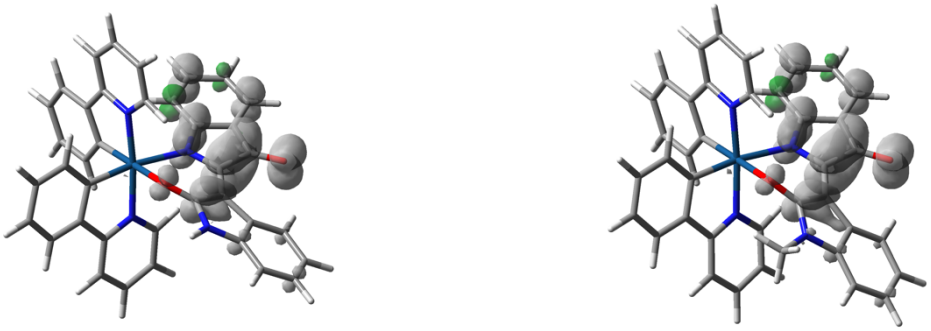

**1** **2**

**Figure S10.** Spin-density distribution of the singly oxidized and singly reduced radicals of **1** and **2** in its fully relaxed geometry, computed by spin-unrestricted DFT in acetonitrile (isovalues: 0.002 e bohr$^{-3}$). In both complexes, the unpaired electron of the oxidized radical is mainly localized on the indirubin ligand (62%), with a minor contribution from the iridium ion (31%); on the other hand, the spin density of the reduced radical is totally confined on the indirubin fragment (>99%).

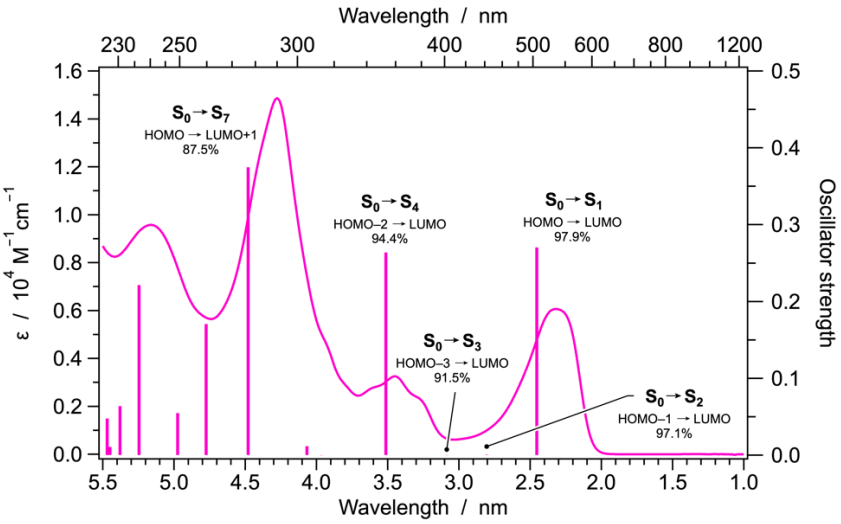


**Figure S11.** Singlet vertical electronic transitions calculated by TD-DFT in acetonitrile for pristine indirubin, compared with its experimental absorption spectrum in the same solvent. The most relevant computed transitions are also described in terms of the predominat pair of molecular orbitals involved in the mono-electronic excitation.

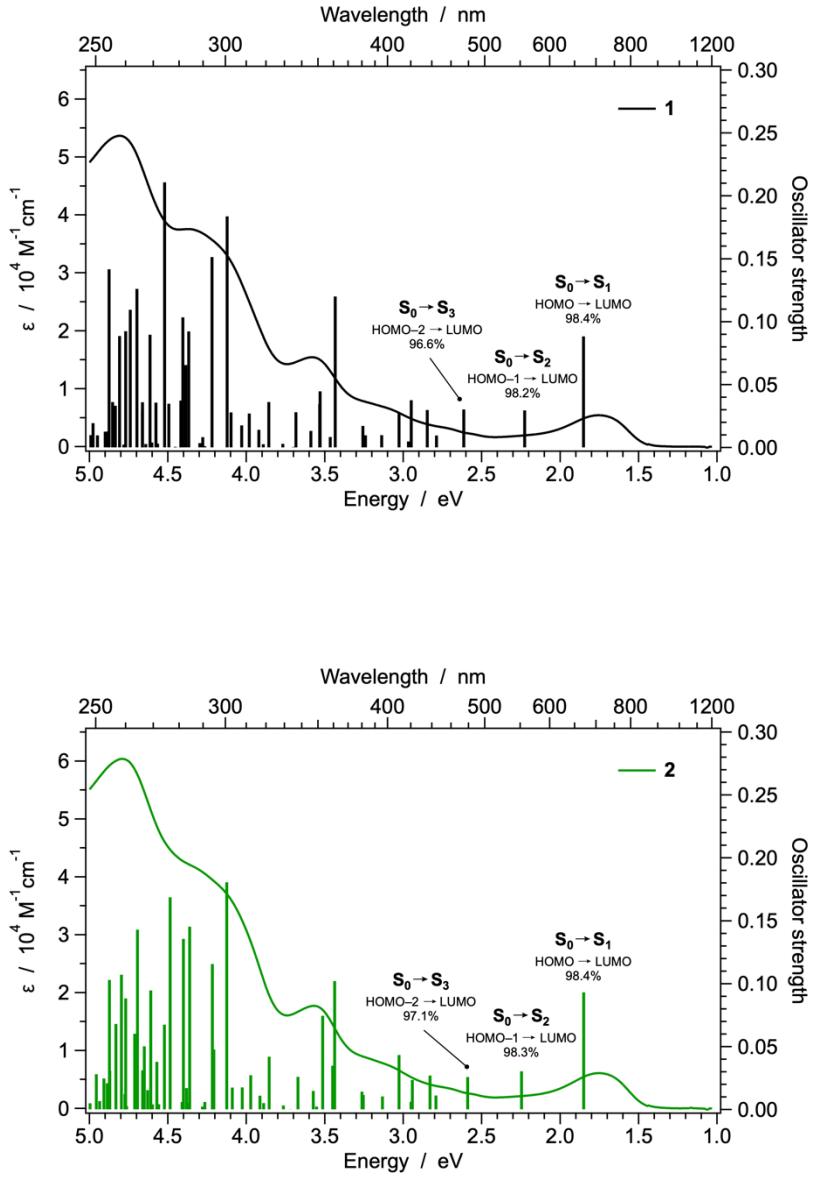


**Figure S12.** Singlet vertical electronic transitions calculated by TD-DFT in acetonitrile for complexes **1** and **2**, compared with its experimental absorption spectrum in the same solvent. The lowest-energy transition is also described in terms of the predominat pair of molecular orbitals involved in the mono-electronic excitation.

**Table S9.** Calculated NTOs couples describing the lowest seven triplet excitations for complex **1** in acetonitrile (see Experimental Section for details). The λ value is the natural transition orbital eigenvalue associated with each NTOs couple; orbital isovalue: 0.04 $e^{-1/2}$ $bohr^{-3/2}$.

| | Transition energy [eV (nm)] | NTO couple hole → electron (λ) | Nature |
|---|---|---|---|
| $S_0 \rightarrow T_1$ | 1.20 (1030) | 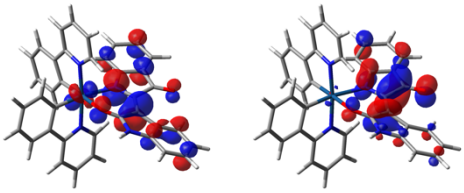 (100%) | mainly centerd on indirubin ligand |
| $S_0 \rightarrow T_2$ | 2.15 (578) | 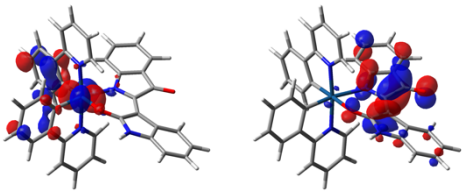 (99.6%) | mainly metal-to-ligand charge transfer from iridium to indirubin |
| $S_0 \rightarrow T_3$ | 2.37 (524) | 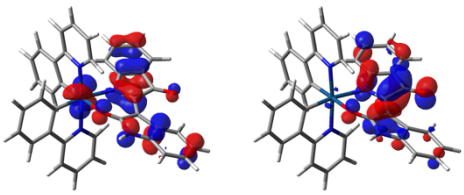 (97.1%) | mixed $^3$LC and $^3$MLCT involving both iridium and indirubin orbitals |
| $S_0 \rightarrow T_4$ | 2.56 (485) | 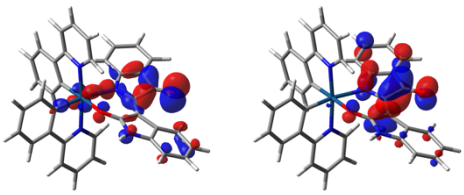 (98.5%) | n–π* on the carbonyl group of the indirubin ligand |
| $S_0 \rightarrow T_5$ | 2.60 (476) | 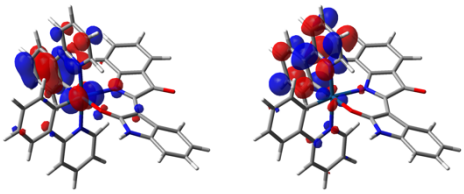 (89.7%) | mainly centerd on cyclometalating ligands |
| $S_0 \rightarrow T_6$ | 2.69 (461) | 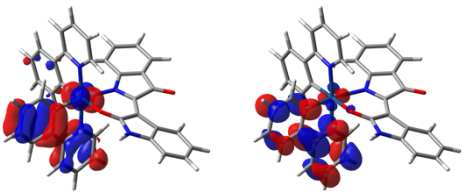 (81.4%) | mainly centerd on cyclometalating ligands |

| | | | | | |
|---|---|---|---|---|---|
| $S_0 \rightarrow T_7$ | 2.74 | (453) | 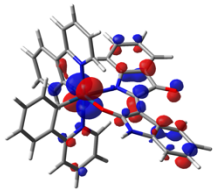 | 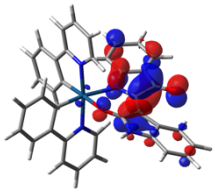 | metal-to-ligand charge transfer from iridium to indirubin |
| | | | (93.1%) | | |

**Table S10.** Calculated NTOs couples describing the lowest seven triplet excitations for complex **2** in acetonitrile (see Experimental Section for details). The λ value is the natural transition orbital eigenvalue associated with each NTOs couple; orbital isovalue: 0.04 $e^{-1/2}$ $bohr^{-3/2}$.

| | Transition energy [eV (nm)] | NTO couple hole → electron (λ) | | Nature |
|---|---|---|---|---|
| $S_0 \rightarrow T_1$ | 1.20 (1033) | 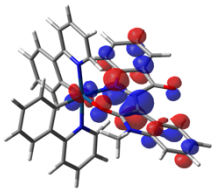 | 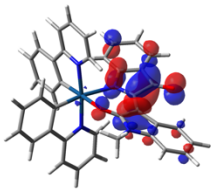 | mainly centerd on indirubin ligand |
| | | (100%) | | |
| $S_0 \rightarrow T_2$ | 2.17 (573) | 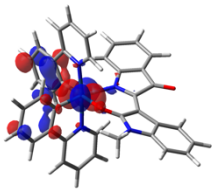 | 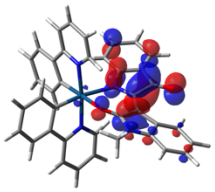 | mainly metal-to-ligand charge transfer from iridium to indirubin |
| | | (99.6%) | | |
| $S_0 \rightarrow T_3$ | 2.35 (527) | 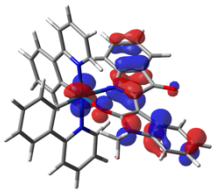 | 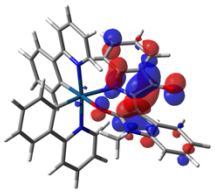 | mixed $^3$LC and $^3$MLCT involving both iridium and indirubin orbitals |
| | | (97.2%) | | |
| $S_0 \rightarrow T_4$ | 2.56 (485) | 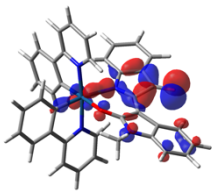 | 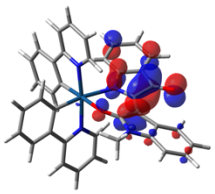 | n–π* on the carbonyl group of the indirubin ligand |
| | | (98.4%) | | |

| | | | | | |
|---|---|---|---|---|---|
| $S_0 \rightarrow T_5$ | 2.60 | (478) | 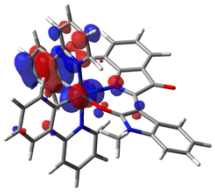 | 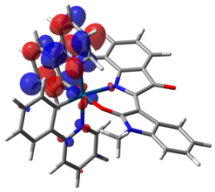 | mainly centerd on cyclometalating ligands |
| | | | (90.1%) | | |
| $S_0 \rightarrow T_6$ | 2.69 | (461) | 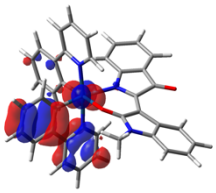 | 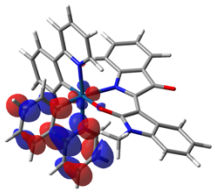 | mainly centerd on cyclometalating ligands |
| | | | (82.3%) | | |
| $S_0 \rightarrow T_7$ | 2.74 | (452) | 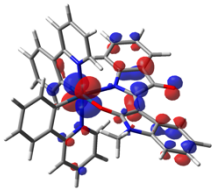 | 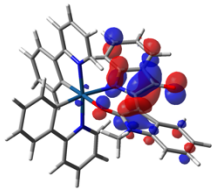 | metal-to-ligand charge transfer from iridium to indirubin |
| | | | (93.2%) | | |

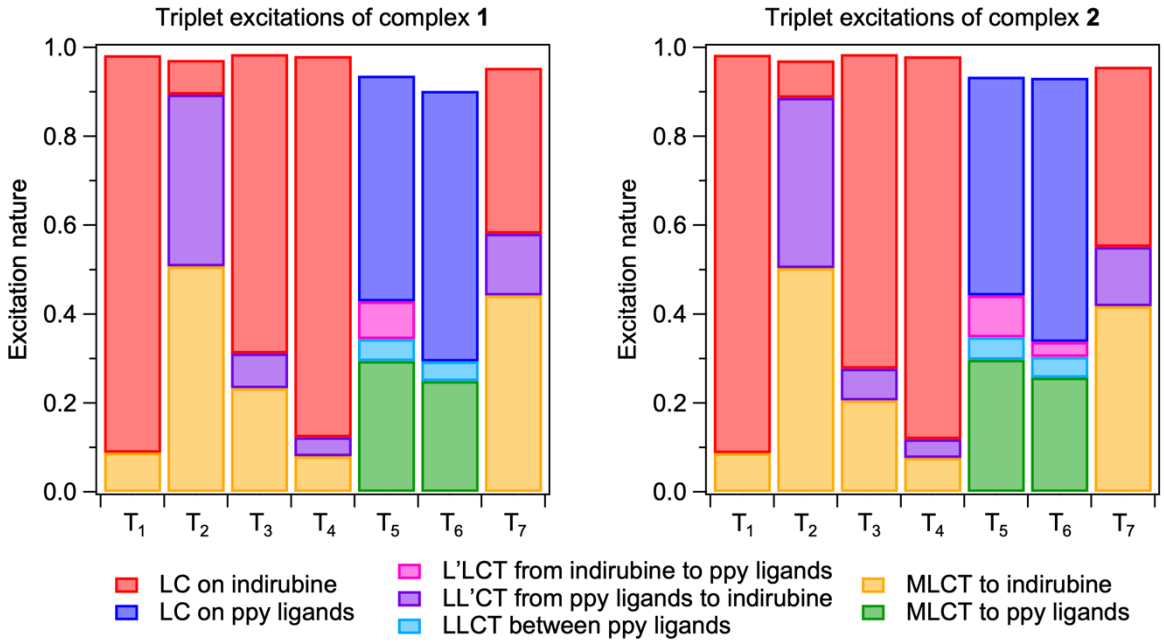


**Figure S13.** Fragment-based analysis of the excited-states reported in Tables S9 and S10, calculated for complexes **1** and **2**, respectively, using TheoDORE software. The complexes were divided into 4 fragments: the iridium ion, the two cyclometalating ligands and the indirubin one. Only contributions above 3% are reported in the bar plots.

## Kinetic model for ultrafast transient-absorption data

All transient absorption matrixes **M** (m × n, in the format: m spectra × n time_delays) have been analyzed by means of singular-value decomposition (SVD):

$$\underset{(m\times n)}{\mathbf{M}} = \underset{(m\times m)}{\mathbf{U}} \times \underset{(m\times n)}{\mathbf{\Sigma}} \times \underset{(n\times n)}{\mathbf{V^*}}$$

The number of the excited-state species have been determined on the basis of the relative value of the diagonal elements of the **Σ** matrix that are above the noise threshold (*i.e.*, 2 for all both the transient-absorption matrix **M** of both complexes **1** and **2**). Accordingly, a model involving two excited-state species is assumed, in which all species are populated by a purely consecutive kinetic scheme:

$$S_0 \xrightarrow{\text{laser pulse}} T_{1-III} \xrightarrow{k_1} T_{1-I} \xrightarrow{k_2} S_0$$

where $S_0$ denotes the ground state, $T_{1\text{-}III}$ is the highest triplet sublevel of the lowest tripet state of the complexes, and $T_{1\text{-}I}$ refres to the same triplet state after equilibration (*i.e.*, with the predominant population of the lowest sublevel I). The laser pulse is assumed to have a Gaussian temporal profile and the $k_n$ values are the first-order kinetic constant modelling the mono-exponential deactivations of the $T_1$ sublevels.

Once the number of principal components was determined (*i.e.*, 2), the experimental transient absorption matrix **M** could be approximated to **M'** and the corresponding SVD matrixes cut to rank 2:

$$\underset{(m\times n)}{\mathbf{M}} \approx \underset{(m\times n)}{\mathbf{M'}} = \underset{(m\times 2)}{\mathbf{U'}} \times \underset{(2\times 2)}{\mathbf{\Sigma'}} \times \underset{(2\times n)}{\mathbf{V'^*}}$$

In order to get physically-meaningful results, the two singular vectors of **V'*** (associated to the temporal evolution of the two singular spectra in **U'**) have been linearly transformed using a square matrix **R** and its inverse $\mathbf{R^{-1}}$, according to the formula:

$$\mathbf{M'} = (\mathbf{U'} \times \mathbf{\Sigma'}) \times \mathbf{I} \times \mathbf{V'^*} = [(\mathbf{U'} \times \mathbf{\Sigma'}) \times \mathbf{R}] \times [\mathbf{R^{-1}} \times \mathbf{V'^*}]$$

The elements of the matrix **R** have been determined by a global-fitting procedure, carried out on the $v_n$ singular vectors of **V'*** (*i.e.*, the principal kinetics of the reduced transient matrix **M'**), solving the equations:

$$\begin{cases} v_1(t) = A_1 \cdot f(t) + B_1 \cdot g(t) \\ v_2(t) = A_2 \cdot f(t) + B_2 \cdot g(t) \end{cases}, \quad \text{so that} \quad \mathbf{R} = \begin{bmatrix} A_1 & B_1 \\ A_2 & B_2 \end{bmatrix}$$

where f(t) is a normalized function obtained by the convolution of a gaussian function simulating the laser excitation pulse (centered at $t_0$ and having σ standard deviation) and a mono-exponential decay function (with $k_1$ kinetic constant), according to the following integral:

$$f(t) = \int_0^{+\infty} e^{-k_1 \cdot \tau} \cdot e^{-\frac{((t-\tau)-t_0)^2}{2\cdot\sigma^2}} d\tau$$

and g(t) is again a normalized function obtained as a convolution of the above-mentioned function and a second mono-exponential decay function (with $k_2$ kinetic constant):

$$g(t) = \int_0^{+\infty} e^{-k_2 \cdot \tau} \cdot f(t-\tau)\, d\tau$$

As a consequence, the global fitting procedure used 4 shared variables [*i.e.*, $t_0$ and σ (depending on the laser pulse), and $k_1$ and $k_2$ kinetic constants (specific of the excited-state dynamics of the sample)] and 4 vector-specific variables [*i.e.*, $A_1$, $B_1$ and $A_2$, $B_2$].

In simple words, each of the two singular vectors of **V'*** (*i.e.*, $v_1(t)$ and $v_2(t)$) has been fitted as a linear combination of two physically meaningful time-profiles (*i.e.*, f(t) and g(t)), in order to allow the transformation of the principal spectra (*i.e.*, the scaled singular vectors **U'** × **Σ'**) in decay-associated spectra (DAS).

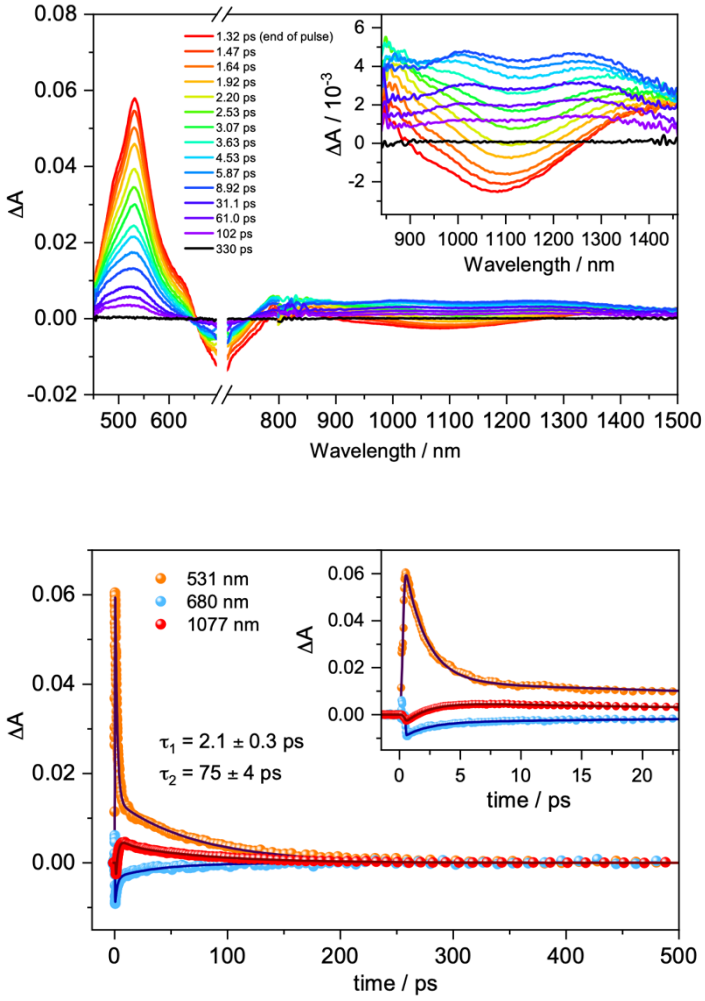


**Figure S14.** Ultrafast transient-absorption data for complex **2** in acetonitrile solution at 298 K; excitation wavelength: 700 nm; pump energy: 4 μJ/pulse; $A_{700nm}$ = 1.0 in a cuvette with 2.00-mm optical path. (Top) Evolution of the transient-absorption spectra at different time delays; inset: amplification of the NIR region. (Bottom) ΔA time evolutions (dots) and fittings (lines) at the indicated wavelengths; inset: amplification in time range between 0 and 23 ps.

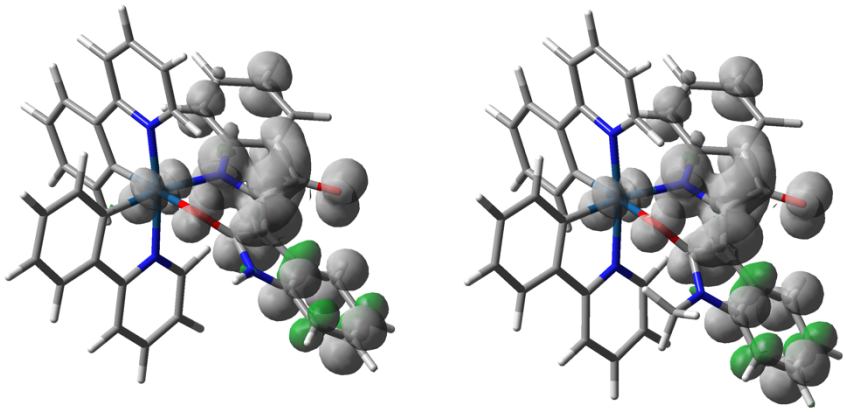

**Figure S15.** Spin-density distribution of the lowest triplet state ($T_1$) of complexes **1** (left) and **2** (right) in its fully relaxed geometry, computed by spin-unrestricted DFT in acetonitrile (isovalues: 0.002 e bohr$^{-3}$). The $T_1$ state is basically a $^3$LC triplet centered on the indirubin ligand, as proved by the atomic spin density distribution, which is 1.86–1.85 e$^-$ on the indirubin ligand (93%), and just 0.12–0.13 e$^-$ on the iridium ion (6%) and 0.02 e$^-$ on the cyclometalating ligands (1%), for complexes **1**–**2**, respectively.

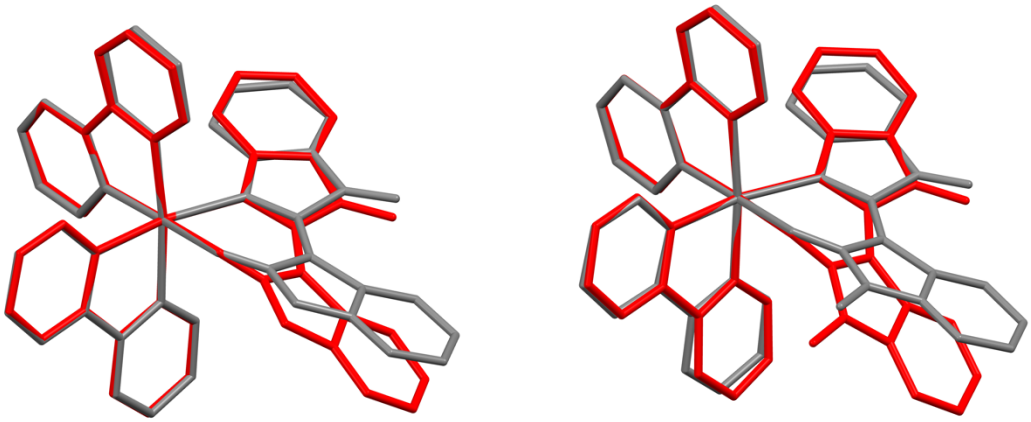

**Figure S16.** Structural overlap (H atoms omitted for clarity) between the minimum-energy geometry of complexes **1** (left) and **2** (right) in their ground state ($S_0$, grey) and in their lowest triplet excited state ($T_1$, red). Both complexes experience a remarkable excited-state distorsion of the indirubin ligand, more evident on the isatin fragment.